Salicylihalamides A and B, Novel Cytotoxic Macrolides from the Marine Sponge *Haliclona* sp.

Karen L. Erickson,[1] John A. Beutler, John H. Cardellina II, and Michael R. Boyd*

Laboratory of Drug Discovery Research and Development, Developmental Therapeutics Program, Division of Cancer Treatment, Diagnosis, and Centers, National Cancer Institute-FCRDC, Building 1052, Room 121, Frederick, Maryland 21702-1201

Received August 20, 1997[⊗]

Two novel, highly potent, cytotoxic macrolides, salicylihalamides A (**1**) and B (**2**), were isolated from the sponge *Haliclona* sp. This new macrolide class incorporates salicylic acid, a 12-membered lactone ring, and an enamide side chain. COMPARE pattern-recognition analyses of the NCI 60-cell mean graph screening profiles of **1** did not reveal any significant correlations to the profiles of known antitumor compounds in the NCI's "standard agent database", thus supporting the conclusion that the salicylihalamides represent a potentially important new class for antitumor lead optimization and in vivo investigations.

Introduction

Sponges of the genus *Haliclona* are well-known for producing a variety of secondary metabolites, most commonly bioactive alkaloids.[2] In our screening of crude extracts for differential cytotoxicity, the organic extract of an Australian collection of an unidentified species of *Haliclona* (phylum Porifera, class Demospongiae, order Haplosclerida, family Haliclonidae) displayed a potent and unique differential cytotoxicity profile in the NCI 60-cell line human tumor assay.[3] Bioassay-guided fractionation of this extract afforded salicylihalamide A (**1**), a novel salicylate macrolide with a highly unsaturated amide side chain. We report herein the structure elucidation of this unusual metabolite and its geometrical isomer, **2**.

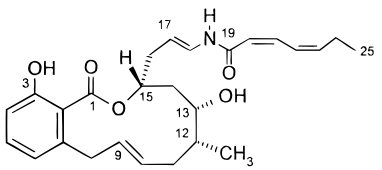

1
2 17Z

Results and Discussion

Salicylihalamide A (**1**) was an amorphous solid whose molecular formula was established as $C_{26}H_{33}NO_5$ by HREIMS. The ^{13}C and DEPT NMR spectra (Table 1) showed 26 unique resonances: 5 quaternary, 14 methine, 5 methylene, and 2 methyl carbons. Chemical shift values further characterized two ester or amide carbonyls, 14 olefinic or aromatic carbons, and two oxygenated methines. Three exchangeable protons completed the proton count. The IR spectrum confirmed OH and/or NH (3288 cm^{-1}) functionalities and suggested the presence of both an amide (1651 cm^{-1}) and an intramolecularly hydrogen-bonded conjugated ester (1697 cm^{-1}).

Because of the sensitivity of **1** to $CDCl_3$ (see Experimental Section), all NMR spectroscopy experiments were carried out in C_6D_6 or CD_3OD. Signals obscured by or unresolved in one solvent were readily discernible in the other. Consequently, $^1H-^1H$ COSY, HMQC, and HMBC NMR data were gathered in both solvents. From a combination of HMQC (Table 1) and COSY[4] spectral data, the following partial structures were generated:

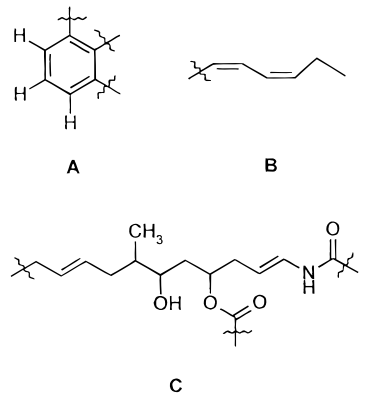

The enamide functionality in segment **C** was identified through a 10.8 Hz coupling between the adjacent olefinic

[⊗] Abstract published in *Advance ACS Abstracts,* November 1, 1997.

(1) On leave from the Carlson School of Chemistry, Clark University, Worcester, MA.

(2) (a) Faulkner, D. J. *Nat. Prod. Rep.* **1993**, *10*, 497−539 and references therein. (b) Parameswaran, P. S.; Kamat, S. Y.; Chandramohan, D.; Nair, S.; Das, B. *Oceanogr. Indian Ocean* **1992**, 417−420 (*Chem. Abstr.* **1994**, *120*, 187482v). (c) Jaspars, M.; Pasupathy, V.; Crews, P. *J. Org. Chem.* **1994**, *59*, 3253−3255. (d) Venkateswarlu, Y.; Reddy, M. V. R.; Rao, J. V. *J. Nat. Prod.* **1994**, *57*, 1283−1285. (e) Kobayashi, M.; Chen, Y.-J.; Aoki, S.; In, Y.; Ishida, T.; Kitagawa, I. *Tetrahedron* **1995**, *51*, 3727−3736. (f) Zeng, Z.; Zeng, L.; Su, J. *Zhongguo Haiyang Yaowu* **1995**, *14*, 5−7 (*Chem. Abstr.* **1995**, *123*, 193621). (g) Shen, Y.-C.; Tai, H.-R.; Duh, C.-Y. *Chin. Pharm. J.* (*Taipei*) **1996**, *48*, 1−10 (*Chem. Abstr.* **1996**, *125*, 82280). (h) Charan, R. D.; Garson, M. J.; Brereton, I. M.; Willis, A. C.; Hooper, J. N. A. *Tetrahedron* **1996**, *52*, 9111−9120.

(3) (a) Boyd, M. R. In *Cancer: Principles and Practice of Oncology Updates*; DeVita, V. T., Jr., Hellman, S., Rosenberg, S. A., Eds.; Lippincott: Philadelphia, 1989; Vol. 3, No. 10; pp 1−12; (b) Boyd, M. R. In *Anticancer Drug Development Guide: Preclinical Screening, Clinical Trials and Approval*; Teicher, B., Ed.; Humana Press: Inc., Towata, NJ, 1997; p 23−42. (c) Boyd, M. R.; Paull, K. *Drug Dev. Res.* **1995**, *34*, 91−109. (d) Weinstein, J. N.; Myers, T. G.; O'Connor, P. M.; Friend, S. H.; Fornace, A. J., Jr.; Kohn, K.; Fojo, T.; Bates, S. E.; Rubinstein, L. V.; Anderson, N. L.; Buolamwini, J. K.; van Osdol, W. W.; Monks, A. P., Scudiero, D. A.; Sausville, E. A.; Zaharevitz, D. W.; Bunow, B.; Viswanadan, V.N.; Johnson, G. W.; Wittes, R. E.; Paull, K. D. *Science* **1997**, *275*, 343−349.

(4) The $^1H-^1H$ COSY spectrum of **1** in C_6D_6 revealed the following correlations (H/H): 4/6, 5/6, 8a/8b, 8a/9, 8a/10, 8a/11b, 8b/9, 9/10, 10/11a, 10/11b, 11a/11b, 11a/12, 11b/12, 12/13, 12/26, 13/14a, 13/14b, 14a/14b, 14a/15, 14b/15, 15/16a, 15/16b, 16a/16b, 16a/17, 16a/18, 16b/17, 16b/18, 17/18, 18/NH, 20/21, 20/22, 20/23, 21/22, 21/23, 22/23, 22/24, 23/24, 24/25.

S0022-3263(97)01556-9 CCC: $14.00

Table 1. ^{13}C (125 MHz) and ^{1}H (500 MHz) NMR Data for Salicylihalamide (1) in C_6D_6 and CD_3OD

C no.	δ_c (C_6D_6)	δ_H (multiplicity, Hz) (C_6D_6)[a]	HMBC (^1H) correlation (C_6D_6)	δ_c (CD_3OD)	δ_H (multiplicity, Hz) (CD_3OD)[a]	HMBC (^1H) correlation (CD_3OD)
1	171.2	–	15	171.0	–	15
2	114.7[b]	–	4, 6, 8a, 8b	123.0	–	6
3	163.0	–	4 and/or 5	157.1	–	5
4	117.1	6.97 (m)	5, 6	115.3	6.72 (d, 7.3)	6
5	134.0	6.97 (m)	6	131.6	7.12 (t, 7.3)	–
6	123.6	6.48 (dd, 6.4, 2.0)	4 and/or 5, 8a, 8b	122.5	6.65 (d, 7.3)	4, 8b
7	142.6	–	5, 6, 8a, 8b, 9	140.7	–	5, 8b
8	39.3	3.32 (br d, 16.6), 3.61 (br dd, 16.6, 4.9)	9	38.8	3.34 (br dd, 16.6, 7.8), 3.56 (dd, 16.6, 8.3)	6, 9, 10
9	132.7	5.28 (dt, 15.1, 4.9, 4.4)	8a, 8b, 11a, 11b	130.7	5.29 (dddd, 15.2, 8.3, 7.8, 1.5)	8b, 11b
10	127.0	5.05 (br m)	8a, 8b, 11a, 11b	131.7	5.36 (m)	8b, 11a
11	38.5	1.65 (dd, 13.7, 8.8), 2.12 (m)	9, 13, 26	38.9	1.75 (m), 2.28 (m)	9, 10
12	37.6	1.51 (br dq, 6.8, 3.5)	11a, 13, 14b, 26	38.6	1.87 (br m)	–
13	70.5	3.46 (dd, 8.8, 3.5)	14a, 15, 26	72.0	4.12 (dd, 9.3, 3.4)	14a, 15
14	35.4	1.28 (dd, 15.0, 8.8), 1.66 (dd, 15.0, 10.3)	13, 15, 16a, 16b	36.6	1.37 (dd, 15.3, 9.3), 1.75 (m)	13, 15, 16
15	75.3	5.55 (dt, 10.3, 6.5)	13, 14b, 16a, 16b, 17	76.0	5.36 (m)	13, 14b, 16
16	36.3	2.07 (ddd, 14.6, 7.3, 6.5), 2.20 (ddd, 14.6, 7.3, 6.5)	14b, 15, 17	37.6	2.39 (ddd, 14.2, 6.8, 6.3), 2.42 (ddd, 14.2, 6.8, 6.3)	15, 17
17	107.0	4.84 (dt, 14.5, 7.3)	15, 16a, 16b	110.4	5.36 (m)	15, 16
18	126.0	7.13 (dd, 14.5, 10.8)	16a, 16b, 17	126.2	6.80 (d, 14.7)	16
19	162.9	–	20, 21, NH	165.9	–	20, 21
20	119.6	5.17 (d, 11.2)	–	120.3	5.68 (d, 11.7)	–
21	136.9	6.62 (dt, 11.2, 1.0)	20, 23	137.7	6.87 (dt, 11.7, 1.0)	23
22	124.9	7.92 (dt, 10.8, 1.5)	20, 24	125.3	7.30 (dt, 10.7, 1.5)	20, 24
23	141.7	5.63 (ddddd, 10.8, 7.3, 7.3, 1.0, 1.0)	21, 24, 25	142.6	5.82 (ddddd, 10.7, 7.4, 7.4, 1.4, 1.0)	21, 24, 25
24	20.8	1.97 (d quintets, 7.3, 7.3, 7.3, 7.3, 1.5)	23, 25	21.5	2.28 (d quintets, 7.4, 7.4, 7.4, 7.4, 1.5)	22, 23, 25
25	14.0	0.77 (t, 7.3)	23, 24	14.4	1.02 (t, 7.4)	23, 24
26	13.9	0.82 (d, 6.8)	11a, 13	13.6	0.85 (d, 6.8)	11b, 13
NH	–	6.76 (d, 10.8)	–	–	–	–
OH (C−3)	–	11.46 (br s)	–	–	–	–

[a] With geminal protons, the smaller δ-value is given the "a" designation, the larger δ-value is given the "b" designation. [b] Weak and broad.

and amide N−H protons; the latter was characterized by its variable chemical shift values. All 26 carbons were accounted for in partial structures **A**−**C**. In the HMBC spectra (Table 1), coupling between the two vinyl hydrogens [δ 5.17 (H-20) and 6.62 (H-21) in C_6D_6; δ 5.68 and 6.87 in CD_3OD] of the hexadiene substructure **B** and the amide carbonyl (δ 162.9 in C_6D_6 and δ 165.9 in CD_3OD) of substructure **C** established the connection of **B** to **C** through this amide carbonyl carbon. This was confirmed by an HMBC correlation between the amide proton and carbonyl in C_6D_6 and by the base peak in the mass spectrum (*m*/*z* 109, C_7H_9O). The IR spectral evidence that the ester carbonyl was both conjugated and intramolecularly hydrogen-bonded (1697 cm^{-1}) was supported by the low field chemical shift of the phenolic OH (δ 11.46, C_6D_6). This indicated that the ester carbonyl was *ortho* to the phenolic OH in substructure **A**. The remaining open aromatic position would then have to be occupied by the allylic carbon of moiety **C**, giving macrolide **1** as the final planar structure for salicylihalamide.

Confirmation of the aromatic substitution pattern came from HMBC correlations, which were optimized for 8.3 Hz couplings. In CD_3OD, the phenolic carbon and the amide carbonyl carbon were resolved, as were all three aromatic protons and all six aromatic carbons. Moreover, the latter were not obscured by solvent resonances. In CD_3OD, the aromatic proton at δ 7.12 (H-5) showed a correlation to both the oxygen-bearing phenolic carbon at δ 157.1 (C-3) and the quaternary aromatic carbon at δ 140.7 (C-7). As this δ 7.12 proton is a triplet (J = 7.3 Hz) in the ^1H NMR spectrum, the two quaternary aromatic carbons to which it is correlated should be *meta* to it. The δ 6.65 (H-6) aromatic hydrogen showed correlation to two different aromatic carbons, the methine at δ 115.3 (C-4) and the quaternary carbon at δ 123.0 (C-2). Furthermore, the δ 6.65 proton was correlated to the side-chain aliphatic carbon at δ 38.8 (C-8), necessitating the placement of this side chain *ortho* to the δ 6.65 hydrogen. To accommodate an *ortho* substituent and account for its chemical shift, this δ 6.65 hydrogen must be *para* to the phenolic OH. Confirming this assignment were the correlations observed between the benzylic proton (H-8, δ 3.56) of the side chain and both the quaternary aromatic carbon at δ 140.7 (C-7) and the δ 122.5 (C-6) aromatic carbon bearing the δ 6.65 hydrogen. The only remaining aromatic site for the ester carbonyl attachment is that *ortho* to the phenolic OH (at δ 123.0), as shown in structure **1**. Additional HMBC correlations are found in Table 1.

The relative stereochemistry of salicylihalamide A (**1**) was deduced from a combination of $^1H-^1H$ coupling constants and difference NOE spectra (Table 1, Figure 1). Figure 1 illustrates important NOE interactions; most notable were the interactions of the alcohol methine (H-13) with the ester methine (H-15), the methyl-bearing methine (H-12), and the olefinic hydrogen (H-10). All four of these protons must reside on the same face of the molecule, leading to the relative stereochemistry depicted in Figures 1 and 2. The dihedral angle between the ester methine (H-15) and H-14a must be approximately 90°, since no coupling was observed between these two vicinal hydrogens. The dihedral angle between H-15 and H-14b must approach 180° to accommodate both their coupling constant (10.3 Hz) and the lack of a measurable NOE between them. Likewise, H-14b and the alcohol methine (H-13) showed no measurable coupling, indicating a

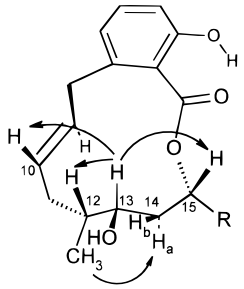

Figure 1. Selected NOE relationships in **1**.

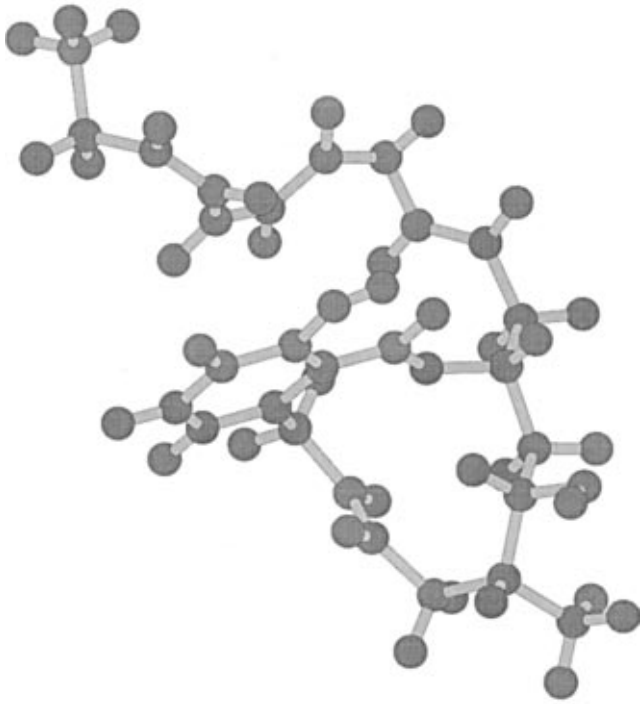

Figure 2. Computer-generated model of the conformation of **1**.

dihedral angle of approximately 90°, while a large dihedral angle between H-14a and H-13 was needed to accommodate a sizable coupling (8.8 Hz). H-13, in turn, displayed a *J*-value of 3.5 Hz and a substantial NOE with H-12, suggesting a dihedral angle of approximately 60° between these two protons. Molecular modeling studies, generating minimum energy structures with the NOE constraints described above, gave rise to predicted *J*-values that agreed within 1−1.5 Hz of the actual experimental values. Figure 2 depicts one such computer-generated model of salicyclihalamide A.

The question of absolute stereochemistry was addressed through the use of Mosher esters.[5] Both the (*R*)- and (*S*)-methoxy trifluoromethylphenyl acetate (MTPA) diesters of **1** were prepared and subjected to ^{1}H NMR analysis (Table 2).[6] The C-12 methyl hydrogens (H-26) and H-10 of the (*R*)-derivative appeared upfield of those

(5) (a) Ohtani, I.; Kusumi, T.; Kashman, Y.; Kakisawa, H. *J. Org. Chem.* **1991**, *56*, 1296−1297. (b) Dale, J. A.; Mosher, H. S. *J. Am. Chem. Soc.* **1973**, *95*, 512−519. For more recent applications see (c) Butler, W. M.; Koreeda, M. *J. Org. Chem.* **1989**, *54*, 4499−4503 and references therein. (d) Leclercq, S.; Thirionet, I.; Broeders, F.; Daloze, D., VanderMeer, R.; Braekman, J. C. *Tetrahedron* **1994**, *50*, 8465−8488. (e) Kaneko, Y.; Matsuo, T.; Kiyooka, S. *Tetrahedron Lett.* **1994**, *35*, 4107−4110.

(6) A small amount of the tris-MTPA derivative (diester imide) was formed in each case and removed by preparative TLC prior to NMR analyses (see Experimental Section).

Table 2. Mosher Ester Analysis of Salicylihalamide A (1) in C_6D_6

	H-10	H-26	H-14a	H-15	H-17
(*R*)-MTPA diester	4.92	0.52	1.58	5.55	4.64
(*S*)-MTPA diester	5.58	0.63	1.52	5.04	4.44
Δ ($\delta_S - \delta_R$)	+0.66	+0.11	−0.06	−0.51	−0.20

of the (*S*)-derivative in C_6D_6 . Likewise, H-14a, H-15, and H-17 appeared downfield in the (*R*)-derivative (**3a**) relative to the (*S*)-derivative (**3b**) in C_6D_6. That H-17 is found on the same face of the molecule as the Mosher ester site could be seen by a strong NOE between H-17 and the ester methine, H-15. Similar results were observed in NMR spectra recorded in CD_3OD. These data allowed the absolute configuration at C-13 to be assigned as *S*. Partial structures **3a** and **3b** depict the classical Mosher drawings accounting for the observed chemical shift differences. In the (*R*,*S*)-diastereomer (**3a**), the H-10 and Me-26 hydrogens experience shielding

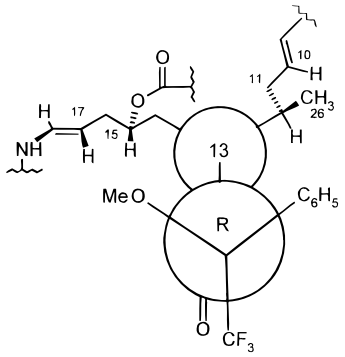

3a

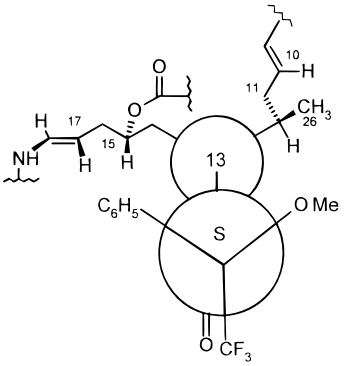

3b

from the phenyl group, while in the (*S*,*S*)-diastereomer (**3b**), H-14a, H-15, and H-17 experience shielding from the phenyl group. If C-13 were of (*R*)-configuration, just the opposite shielding results would be obtained. As the relative stereochemistry of all three chiral centers has been established, assignment of (*S*)-configuration at C-13 conferred the (*R*)-configuration at C-12 and C-15, as shown in **1**.

Accompanying salicylihalamide A in the sponge extract was a minor component whose spectral data were nearly identical with those of **1**. Its structure was determined by careful comparison of ^{1}H, ^{13}C, and ^{1}H−^{1}H COSY NMR data in both C_6D_6 and CD_3OD with those of **1**. The sequence of proton−carbon connectivities was identical with that of **1**. The only significant difference between **1** and its isomer, **2**, was the coupling constant for H-17 and H-18, 10.2 Hz, compared to 14.6 Hz for **1**. Thus, salicylihalamide B (**2**) was the 17-*Z* isomer of **1**.

A search of the literature did not reveal any known compounds of this skeletal type. In a sense, salicylihalamides **1** and **2** would seem more typical of fungal metabolites than sponge metabolites. The closest analogues appear to be the fungal-derived orsellinic acid macrolides such as lasiodiplodin (**4**),[7] which contains a 12-membered benzolactone ring with a methyl substituent at the ester methine. Salicylihalamide also bears

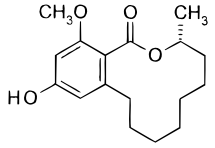

4

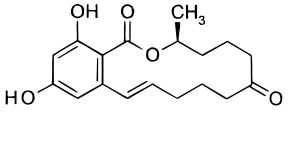

5

some resemblance to zearalenone (**5**), which contains a 14-membered macrolide.[8] However, these relatively simple macrolides lack the enamide side chain of the salicylihalamides, which is reminiscent of, but different from, the enamine formamide residues in the ulapualide[9]/kabiramide[10]/halichondramide[11]/mycalolide[12]/jaspisamide[13] and tolytoxin[14] (scytophycin)/sphinxolide[15] classes of macrolides. The salicylihalamides, then, are novel medium-sized macrolides bearing a highly unsaturated enamide substituent.

Testing of purified **1** in the NCI 60-cell line human tumor screen[3] gave a striking pattern of differential cytotoxicity. This screen provides a powerful tool to assess whether a new compound has the same or similar, or different, mechanism of antitumor action in reference to any known chemical class.[3] COMPARE pattern-recognition analyses of the mean-graph profiles[3b] of **1** did not reveal any significant correlations to the profiles of known antitumor compounds contained in the NCI's standard agent database,[3b] nor did any of the fungal macrolides mentioned above show similar differential cytotoxicity. The mean panel GI_{50} concentration was approximately 15 nM, and the range of differential sensitivity among the 60-cell lines comprising the panel was $\geq 10^3$. As a group, the melanoma cell lines showed the highest average tumor-type subpanel sensitivity (GI_{50} 7 ± 2 nM; TGI 60 ± 25 nM). The salicylihalamides represent an attractive new target for synthetic and mechanism-of-action studies aimed at lead optimization, in vivo investigations, and potential development of a new class of antitumor compound.

Experimental Section

Extraction and Isolation. *Haliclona* sp. was collected by P. Murphy in Southwestern Australia, 0.7 nautical miles off Rottnest Island, in March, 1989, at a depth of 15 m. The sponge reportedly occurred as a green mass with amorphous lobes, growing on the underside of a rocky overhang, and was identified by P. Jane Fromont of James Cook University. A voucher specimen is on deposit at the Smithsonian Institution Taxonomy and Sorting Center, Suitland, MD.

Approximately 450 g frozen wet wt of sponge was ground to a powder with dry ice. The dry ice was allowed to sublime, distilled H_2O was added, and the thawed material was stirred for 3 h at 3 °C and then centrifuged. The marc was freeze-dried and extracted with a mixture of CH_2Cl_2−MeOH (1:1 v/v) at rt overnight. The solvent was removed by filtration and the marc rinsed with MeOH. The combined solutions were evaporated to yield approximately 3.5 g of crude extract.

Initial attempts to isolate the active constituents revealed that the bioactivity was lost from crude extracts and chromatographic fractions thereof in the presence of deuterated chloroform. For example, overnight storage of $CDCl_3$ solutions of partially purified fractions resulted in the formation of a tarry, insoluble residue that was inactive in the in vitro cytotoxicity bioassay. Therefore, all subsequent attempts at isolation avoided the use of chloroform or exposure of samples to $CDCl_3$, and no further problems with decomposition or loss of bioactivity were encountered. Moreover, there was no indication of any instability of the pure isolated compounds in any of the other common organic solvents employed, nor in aqueous or biological media. A typical procedure for efficient isolation and purification of the salicylihalamides from the initial crude extract is as follows.

An aliquot of extract (330 mg) was coated on 2.1 g of diol bonded phase and sequentially batch-eluted with 100 mL aliquots of hexane, CH_2Cl_2, EtOAc, acetone, and MeOH. The cytotoxic CH_2Cl_2 and EtOAc eluates were combined (107 mg) and permeated through Sephadex LH-20 with hexane−toluene−MeOH (3:2:2 v/v, 1.5 × 45 cm column) to yield four fractions, the second of which (8.4 mg) showed NMR signals corresponding to **1**. HPLC on wide-pore C-18 (Rainin 1 × 25 cm) using a linear gradient from 70% to 100% MeOH over 20 min yielded 5.5 mg of **1** (retention time 13 min) and a smaller amount (~0.5 mg) of **2** (retention time 14.5 min). Gratifyingly, TGI- and GI_{50} Compare pattern-recognition analyses (see ref 3c for definitions, details of calculation and interpretation) of the NCI 60-cell mean-graph screening profiles of **1** and the crude extract were highly correlated (e.g., Pearson correlation coefficients ⩾ 0.7), consistent with the presence of the salicylihalamides in the original extract and the basis for initial selection of the extract for bioassay-guided fractionation.

Salicylihalamide A (1). Amorphous solid; $[\alpha]_D$ −35° (c = 0.7, MeOH); λ_{max} (MeOH) 280 nm (ϵ = 34000); ν_{max} (film) 3288, 2964, 1697, 1651, 1606, 1588, 1520, 1464, 1293, 1268, 1247, 1214, 1123, 1068, 972, 869, 735 cm^{-1}; for ^1H and ^{13}C NMR, see Table 1; EIMS m/z 439 [M^+] (43), 421 (1), 410 (5), 409 (2), 392 (2), 330 (7), 315 (8), 313 (3), 312 (3), 296 (10), 288 (12), 278 (4), 231 (12), 191 (40), 149 (17), 125 (18), 124 (6), 109 (100), 108 (19), 107 (16), 96 (63), 91 (10), 83 (31), 82 (50), 81 (87), 79 (35), 56 (27), 55 (24), 43 (14), 18 (19); HREIMS m/z 439.2354 (M^+, calcd for $C_{26}H_{33}NO_5$, 439.2350).

Salicylihalamide B (2). Amorphous solid; $[\alpha]_D$ −73° (c = 0.3, MeOH); λ_{max} (MeOH) 280 nm (ϵ = 38000); ν_{max} (film) 3356, 2964, 2923, 1690, 1651, 1588, 1503, 1463, 1294, 1246, 1212, 1121, 1032, 972 cm^{-1}; ^1H NMR (C_6D_6) δ 0.77 (3H, t, 7.3), 0.83 (3H, d, 6.8), 1.22 (dd, 15.2, 8.8), 1.32 (br s), 1.50 (br q, 6.8), 1.73 (br m), 1.74 (dd, 15.2, 10.5), 1.89 (ddd, 15.2, 7.8, 7.4), 1.95 (2H, quintet, 7.3), 2.05 (ddd, 14.7, 6.8, 6.4), 2.08 (br m), 3.25 (br d, 16.5), 3.27 (br d, 8.8), 3.56 (dd, 16.5, 4.9), 4.52 (dt, 10.2, 8.8, 8.8), 5.08 (ddd, 15.6, 7.3, 6.4), 5.17 (very br m), 5.20 (very br m), 5.48 (d, 11.2), 5.62 (dt, 10.7, 7.8, 7.3), 6.45 (dd, 8.3, 3.9), 6.62 (dd, 11.2, 10.8), 6.95 (m), 7.29 (t, 10.3), 7.66 (br d, 10.2), 7.93 (t, 10.8), 11.58 (br s); ^{13}C NMR (C_6D_6) δ 13.8, 14.0, 20.8, 31.5, 36.2, 38.0, 38.4, 39.4, 70.9, 76.1, 103.3, 117.2, 119.5, 123.7, 124.9, 125.4, 126.8, 132.8, 134.6, 137.4, 141.9, 163.0, 172.0 (3 of the quaternary carbons were not observed); HREIMS m/z 439.2351 (M^+, calcd for $C_{26}H_{33}NO_5$, 439.2350).

Preparation of MTPA Esters. To a mixture of 0.5 mg of **1** in 10 μL of anhydrous CH_2Cl_2 and 15 μL of anhydrous pyridine in a septum-sealed vial were added 1.2 μL of the enantiomerically pure α-methoxy-α-trifluoromethyl phenyl-

(7) Aldridge, D. C.; Galt, S.; Giles, D.; Turner, W. B. *J. Chem. Soc. (C)* **1971**, 1623−1627.

(8) Urry, W. H.; Wehrmeister, H. L.; Hodge, E. B.; Hidy, P. H. *Tetrahedron Lett.* **1966**, 3109−3114.

(9) Roesener, J. A.; Scheuer, P. J. *J. Am. Chem. Soc.* **1986**, *108*, 846−847.

(10) Matsunaga, S.; Fusetani, N.; Hashimoto, K.; Koseki, K.; Noma, M. *J. Am. Chem. Soc.* **1986**, *108*, 847−849.

(11) (a) Kernan, M. R.; Faulkner, D. J. *Tetrahedron Lett.* **1987**, *28*, 2809−2812. (b) Kernan, M. R.; Molinski, T. F.; Faulkner, D. J. *J. Org. Chem.* **1988**, *53*, 5014−5020.

(12) (a) Fusetani, N.; Yasumuro, K.; Matsunaga, S.; Hashimoto, K. *Tetrahedron Lett.* **1989**, *30*, 2809−2812. (b) Rashid, M. R.; Gustafson, K. R.; Cardellina, J. H., II; Boyd, M. R. *J. Nat. Prod.* **1995**, *58*, 1120−1125.

(13) Kobayashi, J.; Murata, O.; Shigemori, H.; Sasaki, T. *J. Nat. Prod.* **1993**, *56*, 787−791.

(14) Carmeli, S.; Moore, R. E.; Patterson, G. M. L. *J. Nat. Prod.* **1990**, *53*, 1533−1542.

(15) D'Auria, M. V.; Paloma, L. G.; Minale, L.; Zampella, A.; Verbist, J.-F.; Roussakis, C.; Debitus, C. *Tetrahedron* **1993**, *49*, 8657−8664.

acetyl chloride. The reaction mixture was allowed to stand at 25° for 16 h. H_2O and CH_2Cl_2 were added, and the CH_2Cl_2 layer was washed several times with H_2O and then passed through a short column of anhydrous Na_2SO_4 and evaporated to dryness under N_2. The residue was subjected to reverse-phase TLC (C_{18}) with MeOH to give di- and tri-MTPA derivatives.

Diesters: HRFABMS *m/z* 872.324 [(*R*)-derivative]; 872.323 [(*S*)-derivative] (MH^+, calcd for $C_{46}H_{48}F_6NO_9$, 872.322).

Diester Imides: HRFABMS *m/z* 1088.361 [(*R*)-derivative]; 1088.362 [(*S*)-derivative] (MH^+, calcd for $C_{56}H_{55}F_9NO_{11}$, 1088.362).

Computer Modeling. Calculations were performed using Macromodel v3.0[16] implemented on a VAX 6620. An input model with a flat macrolide structure with relative stereochemistry proposed by Dreiding models was drawn by hand. Distance constraints were applied sequentially, and energy minimization was performed at each step. After constraints corresponding to the prominent observed transannular NOE's had been applied, the constraints were removed and the structure was minimized without constraint to produce the final model. The graphic (Figure 2) was produced by downloading the structure and printing from the Chem3D program.

Cytotoxicity Profile in the NCI 60-Cell Line Screen. Purified **1** was tested in quadruplicate in the NCI in vitro screen,[3] mean-graphs were constructed and averaged, and COMPARE analyses were performed as described.[3c] The averaged, individual negative log GI_{50} values comprising the GI_{50} mean-graph, along with the respective subpanel and cell-line identifiers are as follows: [Leukemia] CCRF−CEM (7.89), HL-60-TB (9.04), K-562 (8.41), MOLT-4 (7.96), RPMI-8226 (7.89), SR (8.44); [Lung] A549/ATCC (8.54), EKVX (7.52), HOP-62 (8.38), HOP-92 (7.77), NCI−H226 (8.80), NCI−H23 (6.55), NCI−H322M (6.72), NCI−H460 (9.01), NCI−H522 (7.26); [Colon] COLO 205 (8.07), HCC-2998 (6.74), HCT-116 (8.74), HCT-15 (8.44), HT29 (8.54), KM12 (8.30), SW-620 (7.54); [Brain] SF-268 (7.55), SF-295 (8.96), SF-539 (7.89), SNB-19 (6.47), SNB-75 (6.21), U251 (7.57); [Melanoma] LOX-IMVI (9.11), MALME−3M (7.62), M14 (8.92), SK-MEL-2 (7.47), SK-MEL-28 (7.00), SK-MEL-5 (9.00), UACC-257 (8.47), UACC-62 (8.38); [Ovary] IGROV1 (7.89), OVCAR-3 (7.03), OVCAR-4 (5.30), OVCAR-5 (8.11), OVCAR-8 (8.43), SK−OV-3 (5.54); [Kidney] 786−0 (7.92), A498 (6.55), ACHN (8.01), CAKI-1 (8.96), RXF-393 (9.07), SN-12C (7.77), TK-10 (5.74), UO-31 (8.31); [Prostate] PC-3 (7.51), DU-145 (8.26); [Breast] MCF-7 (7.12), MCF-7-ADR−RES (8.07), MDA-MB-231/ATCC (6.92), HS-578T (5.85), MDA-MB-435 (7.82), MDA-N (8.00), BT-549 (9.30), T-47D (8.34). The aforementioned screening data are directly amenable to use by investigators who wish to access Compare-search and other pattern-recognition tools and screening databases[3] currently being deployed by the U.S. National Cancer Institute for general use on the Internet (http://epnws1.ncifcrf.gov:2345/dis3d/dtpsearch.html).

Acknowledgment. We gratefully acknowledge the assistance of G. Gray (mass spectroscopy), T. Prather and R. H. Shoemaker (cell culture), T. McCloud (sponge extraction), P. Murphy, the Australian Institute of Marine Sciences, and K. Snader (NPB/DTP) (collection), P. J. Fromont (taxonomy), A. Monks and D. Scudiero (primary antitumor screening), and the Frederick Biomedical Supercomputing Center (modeling facilities and assistance).

Supporting Information Available: Copies of ^1H and ^{13}C NMR and mass spectra of **1** and **2** (6 pages). This material is contained in libraries on microfiche, immediately follows this article in the microfilm version of the journal, and can be ordered from the ACS; see any current masthead page for ordering information.

JO971556G

(16) Mohamadi, F.; Richards, N. G. J.; Guida, W. C.; Liskamp, R.; Lipton, M.; Caufield, C.; Chang, G.; Hendrickson, T.; Still, W. C. *J. Comput. Chem.* **1990**, *11*, 440−467.